

# Energy Transfer from Individual Semiconductor Nanocrystals to Graphene

Zheyuan Chen,<sup>†,5</sup> Stéphane Berciaud,<sup>†,\*,5</sup> Colin Nuckolls,<sup>†</sup> Tony F. Heinz,<sup>‡</sup> and Louis E. Brus<sup>†,\*</sup>

<sup>†</sup>Department of Chemistry and <sup>‡</sup>Departments of Physics and Electrical Engineering, Columbia University, New York, New York 10027. <sup>5</sup>These authors contributed equally to this work.

**ABSTRACT** Energy transfer from photoexcited zero-dimensional systems to metallic systems plays a prominent role in modern day materials science. A situation of particular interest concerns the interaction between a photoexcited dipole and an atomically thin metal. The recent discovery of graphene layers permits investigation of this phenomenon. Here we report a study of fluorescence from individual CdSe/ZnS nanocrystals in contact with single- and few-layer graphene sheets. The rate of energy transfer is determined from the strong quenching of the nanocrystal fluorescence. For single-layer graphene, we find a rate of  $\sim 4 \text{ ns}^{-1}$ , in agreement with a model based on the dipole approximation and a tight-binding description of graphene. This rate increases significantly with the number of graphene layers, before approaching the bulk limit. Our study quantifies energy transfer to and fluorescence quenching by graphene, critical properties for novel applications in photovoltaic devices and as a molecular ruler.

**KEYWORDS:** semiconductor nanocrystals · graphene · energy transfer · charge transfer · fluorescence quenching

**M**etallic surfaces are known to quench the fluorescence from nearby photoexcited dipoles through resonant energy transfer.<sup>1,2</sup> On the other hand, no energy transfer is expected when a dipole is placed in the vicinity of a transparent insulating surface. Graphene,<sup>3–5</sup> as an atomically thin and nearly transparent semimetal represents an intermediate case of both fundamental and practical interest. Indeed, single-layer graphene (SLG) possesses extremely high carrier mobility,<sup>6</sup> while absorbing only  $\sim 2\%$  of incoming light, independent of wavelength across the visible spectrum.<sup>7,8</sup> These properties make graphene an excellent candidate for solar cell electrodes<sup>9</sup> and other applications in photonics. Here we examine the interaction of the 2-dimensional graphene system with another model nanoscale system, that of 0-dimensional semiconductor nanocrystals. Such nanocrystals have broad and size-tunable absorption, and high photostability,<sup>10</sup> which make them promising systems for diverse optical

applications, including the light-harvesting material in photovoltaic cells.<sup>11–13</sup>

Resonant (Förster) energy transfer from nanocrystals to single and few-layer graphene is expected to occur, since these systems exhibit broad absorption across the visible spectral range. SLG, for example, is characterized by a linear band dispersion around the corners of its Brillouin zone (K and K' points)<sup>5</sup> and a nearly constant optical absorption. Near graphene, electronically excited species, such as semiconductor nanocrystals, can thus be quenched by resonant energy transfer, exciting electron–hole pairs in the semimetal.<sup>1</sup> Whether this rate is significant compared with the natural radiative decay is, however, presently unknown. Photoexcited semiconductor nanocrystals can also decay by a competing process of charge transfer to the graphene substrate. Photoinduced electron transfer to graphene would produce charged nanocrystals, which are understood to be responsible for the “off” periods in fluorescence blinking.<sup>14,15</sup> Our measurements of core/shell CdSe/ZnSe nanocrystals adsorbed on single and few-layer graphene (FLG) also explore this potential decay channel.

## RESULTS AND DISCUSSION

Graphene layers were deposited on quartz substrates by mechanical exfoliation<sup>3</sup> of kish graphite. Isolated CdSe/ZnS nanocrystals were then spun cast onto the samples (see Methods for details.) Fluorescence from individual nanocrystals could be observed for nanocrystals located both on the bare quartz substrate and on a graphene layer (Figure 1). Strong fluorescence quenching was observed for particles deposited on graphene sheets com-

\*Address correspondence to leb26@columbia.edu.

Received for review March 11, 2010 and accepted April 15, 2010.

Published online April 19, 2010. 10.1021/nn1005107

© 2010 American Chemical Society

pared to the bare substrate. The integrated fluorescence intensities varied significantly from nanocrystal to nanocrystal, on both quartz and graphene. We first calculated the average quenching factor  $\rho = I^q/I^r$ , where  $I^q$  and  $I^r$  are the fluorescence intensities (expressed in emitted photons per unit time) on quartz and on graphene, respectively. Each isolated diffraction limited fluorescence spot was assigned to an individual nanocrystal and fit to 2D Gaussian profile. Statistical distributions of the integrated intensities were constructed separately for both populations of nanocrystals on quartz and on graphene (Figure 2). The widths of the distributions show a considerable inhomogeneity. The average intensities in Figure 2c,d give a quenching factor of  $\sim 25$  for SLG.

Different “blinking” behavior is observed for nanocrystals on quartz and on graphene (Figure 3). On quartz, long “off” periods occur; these are not observed on graphene. Different blinking behavior leads to different integrated intensities from one nanocrystal to the next, which complicates our quantitative measurement of quenching. Blinking is known to depend upon both the laser intensity<sup>18</sup> and on the nature of the underlying substrate.<sup>16–20</sup> However, nanocrystal fluorescence during the “on” period is known to have a relatively constant radiative rate<sup>21</sup> and near unity quantum yield.<sup>22</sup> Thus, in order to remove the effect of blinking, we used the following procedure to calculate the comparative intensities during the “on” periods only. To remain in the linear regime, a low laser excitation intensity of  $\sim 50$  W/cm<sup>2</sup> was used to probe nanocrystals on quartz. A much shorter nanocrystal excited-state lifetime exists on SLG (Figure 2). We therefore used higher excitation intensity ( $\sim 1500$  W/cm<sup>2</sup>) for nanocrystals on graphene, but with the same binning time (10 ms) for recording the fluorescence emission. The integrated fluorescence signals from nanocrystals on graphene still show a linear relationship with laser intensity at this high value, indicating that the dependence of blinking behavior on excitation intensity is negligible. On quartz the “on” and “off” periods lead to a familiar bimodal distribution of fluorescence intensities<sup>15</sup> (Figure 3b). From a collection of more than 160 time traces on quartz, we found an average ratio of the “on” period  $T_{on}$  to the integration time  $T$  of 0.34. Variations in  $T_{on}$  for different nanocrystals are chiefly responsible for the broad distribution shown in Figure 2d.

In contrast, fluctuations in the fluorescence intensity from nanocrystals on graphene are dramatically reduced. The fluorescence time traces yield a single-modal distribution of intensities (Figure 3b). This suppression of blinking suggests that the fluorescence quenching rate is significantly faster than the photoexcited electron trapping rate responsible for the “off” state. Most of the integration time is “on” for nanocrystals on graphene, and thus on graphene  $T_{on}$  is approximated as  $T$  in Figure 3a. The measured quenching fac-

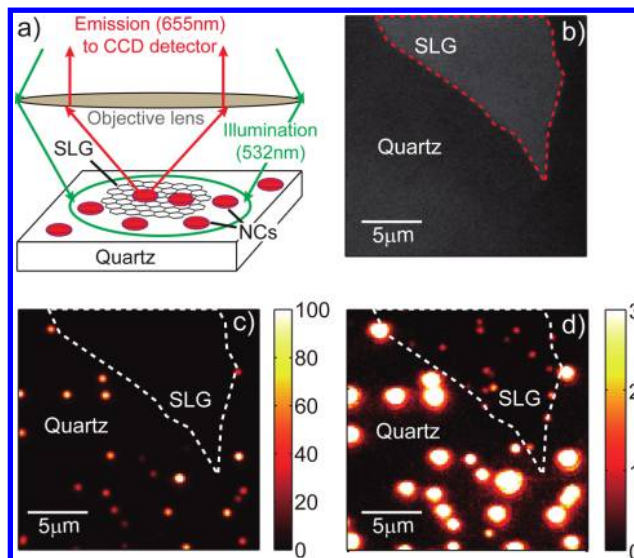


**Figure 1.** Optical and fluorescence images of individual nanocrystals on single-layer graphene and on the quartz substrate. (a) Schematic diagram of our experimental setup; (b) optical reflectivity image in the emission range of our nanocrystals; (c) wide-field fluorescence image of individual CdSe/ZnS nanocrystals in the region shown in panel b. The color scale-bar indicates the number of emitted photons (in arbitrary units) integrated over 30s. (d), Same as panel c but in a color scale divided by a factor of 30 in order to show the emission from nanocrystals on a graphene monolayer.

tors were therefore corrected to account for the different “on” fractions, yielding  $\rho \approx 80$ .

We tentatively assign the quenching process, decreasing the nanocrystal quantum yield during the “on” periods, to resonant (Förster) energy transfer and

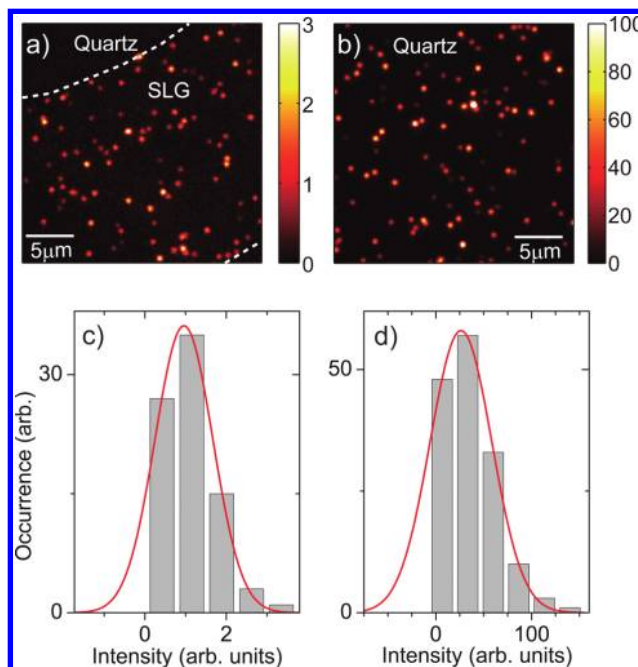


**Figure 2.** Determination of the fluorescence quenching factor. Fluorescence images and corresponding histograms of the integrated fluorescence intensities for nanocrystals on a graphene monolayer (a and c) as compared to a reference taken on a quartz substrate (b and d). The red curves in panels C and D show Gaussian fits to the histograms. The centers of the Gaussian profiles were used to calculate the average fluorescence quenching factors.

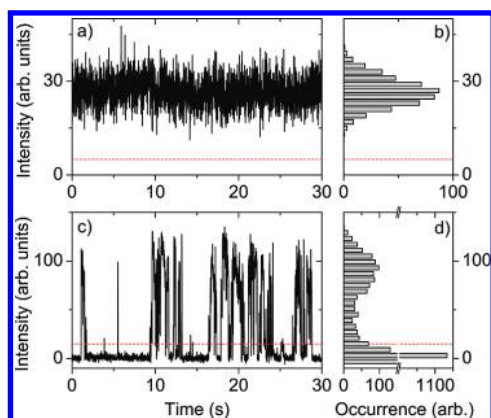


**Figure 3.** Suppression of nanocrystal blinking on single-layer graphene. Fluorescence time traces from an individual nanocrystal lying (a) on a graphene monolayer ( $I_{\text{Laser}} = 1500 \text{ W/cm}^2$ ) and (b) on a quartz substrate ( $I_{\text{Laser}} = 50 \text{ W/cm}^2$ ). Both traces were acquired with a time bin of 10 ms. The dashed horizontal lines indicate the intensity thresholds used to define the “on” and “off” states used in the text. Panels c and d are histograms of the emission intensities corresponding to panels a and b, respectively. After normalization for the laser excitation intensities, we deduce an average fluorescence quenching factor of  $\sim 75$  between the “on” intensity measured on quartz and the intensity measured on graphene.

not electron transfer to graphene. Photoinduced electron transfer from core/shell nanocrystals to doped silicon substrates with a thin surface oxide, and to highly oriented pyrolytic graphite (HOPG), has been studied by electron force microscopy.<sup>23</sup> The rates were quite slow; such charge transfer would be negligible under our conditions of excitation intensity and integration time. In contrast, excited-state resonant energy transfer to graphene is predicted to be efficient as shown below. We express the corrected steady-state quenching factor  $\rho$  (the inverse of the fluorescence quantum yield) in terms of the dipole radiative decay rate  $\gamma_{\text{rad}}$  and nonradiative energy transfer rate  $\gamma_{\text{ET}}$ :  $\rho = (\gamma_{\text{rad}} + \gamma_{\text{ET}})/\gamma_{\text{rad}}$ . We neglect any effects of optical reflection from graphene and also assume the nanocrystal fluorescence quantum yield in the “on” state is unity in the absence of graphene.<sup>22</sup>

The classical theoretical reference for resonant energy transfer from a molecule to a bulk metal is Chance, Prock, and Silbey, which uses the experimental metallic dielectric constant at the emission wavelength.<sup>24</sup> For resonant energy transfer to 2D SLG, we use a theory from Swathi and Sebastian which directly calculates the relevant Coulomb matrix element between the excited molecule and the  $\pi$  electron system of SLG, which is parametrized by the experimentally determined Fermi velocity  $v_{\text{F}}$ .<sup>25,26</sup> (see Supporting Information):

$$\rho(1L) = \frac{\pi}{16} \frac{\alpha}{\epsilon^{5/2}} \left(\frac{c}{v_{\text{F}}}\right)^4 I(z) + 1 \quad (1)$$

$$I(z) = \int_0^1 dt \exp\left(-\frac{2\Delta E z t}{\hbar v_{\text{F}}}\right) \frac{t^3}{\sqrt{1-t^2}}$$

Here  $\alpha$  is the fine structure constant,  $\epsilon$  is the dielectric constant of the surrounding medium,  $c$  is the speed of light in vacuum,  $z$  is the distance from the nanocrystal center to the graphene plane,  $\Delta E = 1.9 \text{ eV}$  is the energy of the emitted photons, and  $v_{\text{F}} = 1 \times 10^6 \text{ ms}^{-1}$  is the Fermi velocity in SLG.<sup>5</sup> We take  $\epsilon$  to be that of the usual coating ligand trioctylphosphine oxide ( $\epsilon = 2.6$ ), and we have also used the standard theoretical expressions for  $\gamma_{\text{rad}}$ .

To our knowledge there is no theoretical expression for the corresponding energy transfer rate in few-layer graphene. Since the interactions between the layers of graphene are relatively weak<sup>5</sup> and we are concerned with excitations in the visible spectral range, we approximate the FLG system simply as a stack of decoupled single-layer graphene sheets. Each layer is treated as an independent energy transfer channel, separated from other layers by the graphite spacing of  $\delta = 0.34 \text{ nm}$ . The dielectric screening from upper-layers of a FLG sample is assumed to be unchanged from that of the nanocrystal ligands. The quenching factor for FLG of  $n$ -layer thickness is then given by

$$\rho(nL) = \frac{\pi}{16} \frac{\alpha}{\epsilon^{5/2}} \left(\frac{c}{v_{\text{F}}}\right)^4 \sum_{i=1}^n I(z_i) + 1 \quad (2)$$

where  $z_i = z_1 + (i-1)\delta$  is the distance from the nanocrystal center to the  $i$ th graphene layer.

A critical parameter in the model is the position of the nanocrystals with respect to the underlying graphene sheets. We measured this height distribution using nanocrystals dispersed on HOPG by tapping-mode atomic-force microscopy (see Supporting Information, Figures S3 and S4). The average height of the top of the nanocrystals was found to be 6.1 nm; thus the average distance from the nanocrystal center to graphene is taken to be  $z_1 \approx 3.05 \text{ nm}$ . From ref 26, the theoretical distance ( $z$ ) dependence of the dipole energy transfer rate to graphene is  $z^{-4}$ . As a result, smaller nanocrystals with lower  $z_1$  should show larger  $\rho$ , and larger nanocrystals with greater  $z_1$  should show smaller  $\rho$ . We do in fact observe a distribution of integrated fluorescence intensities for nanocrystals on graphene (Figure 2b). For SLG we calculated the relative number of emitted photons from each part of the height distribution using eq 1. We found that the total number of emitted photons over the distribution was essentially the same as calculated using the average distance. Thus, in Figure 4 we compare data with theory using the average distance of  $z_1 \approx 3.05 \text{ nm}$ .

The experimental and theoretical quenching factors  $\rho$  are shown in Figure 4. The factors of 70 for SLG and  $\sim 115$  for bilayer graphene are in good agreement with the dipole energy transfer theory in eq 2. This agreement supports assignment of the quenching process to resonant energy transfer and not electron transfer. Considering a typical radiative rate<sup>18,21</sup>  $\gamma_{\text{rad}} \approx 5 \times 10^7$

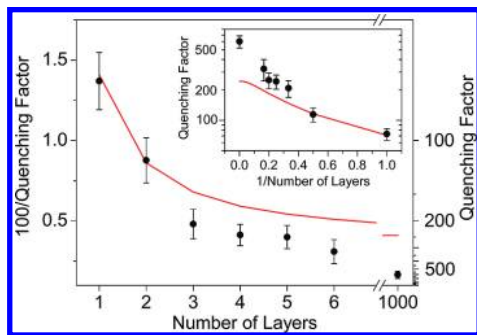


**Figure 4.** Evolution of the fluorescence quenching factor with the number of graphene layers. The black dots represent the quenching factors for single and few-layer graphene and for graphite determined from experiment, with the corresponding experimental uncertainties. The solid lines are the quenching factors calculated from the theory described in the text.

$s^{-1}$ , we estimate  $\gamma_{ET} \approx 4 \times 10^9 s^{-1}$  for SLG. The nanocrystal lifetime on graphene is about 250 ps. Interestingly, this value is similar to the reported near 200 ps $^{-1}$  lifetime of slightly smaller nanocrystals emitting at 620 nm on Au surfaces.<sup>17</sup> We note that in the case of bulk metals, surface roughness is known to cause dramatic modifications in the absorption and radiative decay rates, yielding either fluorescence enhancement or quenching.<sup>17</sup> In the case of atomically thin surfaces like graphene, such effects can be neglected so that a comparison of the fluorescence intensities is equivalent to a comparison of the excited-state lifetime. It is remarkable that nanocrystals on SLG, which only absorbs about 2% of incident light, have roughly the same lifetime as on flat Au metal.

The experimental fluorescence quenching factor  $\rho$  increases with number of layers of the graphene sample, but is not in quantitative agreement with the model. This simple model should increasingly fail as the thickness increases, since it neglects attenuation and reflection of the emitting dipole near field in the top several layers for thick graphene samples.<sup>2</sup> For bulk graph-

ite the measured  $\rho$  is about 600, while the model calculated  $\rho$  is only about 250. In the bulk limit, we can alternatively calculate the expected quenching  $\rho$  using the Persson energy transfer theory for flat bulk materials (see Supporting Information).<sup>1</sup> This theory gives a quenching  $\rho$  of 607, close to our measured value.

## CONCLUSIONS

We have demonstrated efficient energy transfer from individual CdSe/ZnS nanocrystals to single- and few-layer graphene. Our analysis corrects for the differing blinking kinetics observed on quartz and on graphene substrates. The fluorescence intensity of single nanocrystals is quenched by a factor of  $\sim 70$  on single-layer graphene, in agreement with resonant energy transfer theory. The quenching efficiency increases with layer number. Resonant energy transfer is much faster than photoexcited electron transfer for hydrocarbon ligand coated, CdSe/ZnS core/shell nanocrystals adsorbed on graphene.

How might one change the relative rates of electron transfer and energy transfer for solar energy applications? The rate of electron transfer could be increased by strengthening the electronic coupling between nanocrystal and graphene through covalent bonding and by removal of the strongly insulating ZnS outer shell. The photochemical covalent functionalization of graphene has been recently demonstrated,<sup>27</sup> making possible strong electronic coupling between nanocrystals and graphene. The Fermi energy of graphene can also be tuned by electrostatic<sup>28,29</sup> or chemical doping<sup>30</sup> in order to increase the rate of electron transfer and/or decrease the rate of resonant energy transfer.

Note also that, owing to the theoretically predicted  $d^{-4}$  scaling of the rate of energy transfer to 2D SLG,<sup>25,26</sup> fluorescence quenching by graphene should be significant at distances that cannot be reached with normal molecular donor–acceptor pairs,<sup>31</sup> for which energy transfer decreases as  $d^{-6}$ .

## METHODS

Graphene layers were deposited onto clean quartz substrates by mechanical exfoliation<sup>3</sup> of kish graphite (Covalent Materials Corp). The number of graphene layers was determined by both Raman spectroscopy<sup>32</sup> and optical reflection contrast measurements<sup>33</sup> (see Supporting Information). CdSe/ZnS core/shell nanocrystals (Qdot 655, Invitrogen Corp., Cat. No. Q21721MP) were spuncoat onto the substrate at low density ( $<0.4 \mu\text{m}^{-2}$ ). Nanocrystals were illuminated under ambient conditions by a 532-nm continuous-wave diode laser for 30 s at low laser intensity ( $\sim 50 \text{ W/cm}^2$ ). The fluorescence from individual nanocrystals was collected by an air objective (100 $\times$ , NA = 0.9), sent through an emission filter ( $655 \pm 20 \text{ nm}$ ), and imaged onto a CCD array (Figure 1a). Graphene pieces were located under white light illumination. The average fluorescence intensities were corrected for the slight inhomogeneity of the laser beam profile.

**Acknowledgment.** We would like to thank H. Liu, E. Rabani, K. F. Mak, and L. Malard for fruitful discussions. This work was

supported the Department of Energy through the EFRC program (Grant DE-SC00001085) and the Office of Basic Energy Sciences (Grant DE FG02-98ER14861) and by the New York State NYSTAR program.

**Supporting Information Available:** Details of the theoretical calculation of the quenching factors for graphene layers and bulk graphite, Raman spectra and contrast ratio of graphene layers, AFM image of individual CdSe/ZnS nanocrystals on HOPG and histogram of heights. This material is available free of charge via the Internet at <http://pubs.acs.org>.

## REFERENCES AND NOTES

- Persson, B. N. J.; Lang, N. D. Electron-Hole-Pair Quenching of Excited-States near a Metal. *Phys. Rev. B* **1982**, *26*, 5409–5415.
- Barnes, W. L. Fluorescence near Interfaces: The Role of Photonic Mode Density. *J. Mod. Opt.* **1998**, *45*, 661–699.

- Novoselov, K. S.; Jiang, D.; Schedin, F.; Booth, T. J.; Khotkevich, V. V.; Morozov, S. V.; Geim, A. K. Two-Dimensional Atomic Crystals. *Proc. Natl. Acad. Sci. U.S.A.* **2005**, *102*, 10451–10453.
- Geim, A. K.; Novoselov, K. S. The Rise of Graphene. *Nat. Mater.* **2007**, *6*, 183–191.
- Castro Neto, A. H.; Guinea, F.; Peres, N. M. R.; Novoselov, K. S.; Geim, A. K. The Electronic Properties of Graphene. *Rev. Mod. Phys.* **2009**, *81*, 109–162.
- Bolotin, K. I.; Sikes, K. J.; Jiang, Z.; Klima, M.; Fudenberg, G.; Hone, J.; Kim, P.; Stormer, H. L. Ultrahigh Electron Mobility in Suspended Graphene. *Solid State Commun.* **2008**, *146*, 351–355.
- Mak, K. F.; Sfeir, M. Y.; Wu, Y.; Lui, C. H.; Misewich, J. A.; Heinz, T. F. Measurement of the Optical Conductivity of Graphene. *Phys. Rev. Lett.* **2008**, *101*, 196405/1–4.
- Nair, R. R.; Blake, P.; Grigorenko, A. N.; Novoselov, K. S.; Booth, T. J.; Stauber, T.; Peres, N. M. R.; Geim, A. K. Fine Structure Constant Defines Visual Transparency of Graphene. *Science* **2008**, *320*, 1308.
- Wang, X.; Zhi, L. J.; Mullen, K. Transparent, Conductive Graphene Electrodes for Dye-Sensitized Solar Cells. *Nano Lett.* **2008**, *8*, 323–327.
- Nirmal, M.; Brus, L. Luminescence Photophysics in Semiconductor Nanocrystals. *Acc. Chem. Res.* **1999**, *32*, 407–414.
- Huynh, W. U.; Dittmer, J. J.; Alivisatos, A. P. Hybrid Nanorod–Polymer Solar Cells. *Science* **2002**, *295*, 2425–2427.
- Gur, I.; Fromer, N. A.; Geier, M. L.; Alivisatos, A. P. Air-Stable All-Inorganic Nanocrystal Solar Cells Processed from Solution. *Science* **2005**, *310*, 462–465.
- Kamat, P. V. Quantum Dot Solar Cells. Semiconductor Nanocrystals as Light Harvesters. *J. Phys. Chem. C* **2008**, *112*, 18737–18753.
- Nirmal, M.; Dabbousi, B. O.; Bawendi, M. G.; Macklin, J. J.; Trautman, J. K.; Harris, T. D.; Brus, L. E. Fluorescence Intermittency in Single Cadmium Selenide Nanocrystals. *Nature* **1996**, *383*, 802–804.
- Cichos, F.; von Borczyskowski, C.; Orrit, M. Power-Law Intermittency of Single Emitters. *Curr. Opin. Colloid Interface Sci.* **2007**, *12*, 272–284.
- Shimizu, K. T.; Woo, W. K.; Fisher, B. R.; Eisler, H. J.; Bawendi, M. G. Surface-Enhanced Emission from Single Semiconductor Nanocrystals. *Phys. Rev. Lett.* **2002**, *89*, 117401/1–4.
- Ito, Y.; Matsuda, K.; Kanemitsu, Y. Mechanism of Photoluminescence Enhancement in Single Semiconductor Nanocrystals on Metal Surfaces. *Phys. Rev. B* **2007**, *75*, 033309/1–4.
- Fu, Y.; Zhang, J.; Lakowicz, J. R. Suppressed Blinking in Single Quantum Dots (Qds) Immobilized near Silver Island Films (Sifs). *Chem. Phys. Lett.* **2007**, *447*, 96–100.
- Matsumoto, Y.; Kanemoto, R.; Itoh, T.; Nakanishi, S.; Ishikawa, M.; Biju, V. Photoluminescence Quenching and Intensity Fluctuations of CdSe–ZnS Quantum Dots on an Ag Nanoparticle Film. *J. Phys. Chem. C* **2008**, *112*, 1345–1350.
- Yuan, C. T.; Yu, P.; Ko, H. C.; Huang, J.; Tang, J. Antibunching Single-Photon Emission and Blinking Suppression of CdSe/ZnS Quantum Dots. *ACS Nano* **2009**, *3*, 3051–3056.
- Fisher, B. R.; Eisler, H. J.; Stott, N. E.; Bawendi, M. G. Emission intensity dependence and single-exponential behavior in single colloidal quantum dot fluorescence lifetimes. *J. Phys. Chem. B* **2004**, *108*, 143–148.
- Brokmann, X.; Coolen, L.; Dahan, M.; Hermier, J. P. Measurement of the radiative and nonradiative decay rates of single CdSe nanocrystals through a controlled modification of their spontaneous emission. *Phys. Rev. Lett.* **2004**, *93*, 107403/1–4.
- Li, S.; Steigerwald, M. L.; Brus, L. E. Surface States in the Photoionization of High-Quality CdSe Core/Shell Nanocrystals. *ACS Nano* **2009**, *3*, 1267–1273.
- Chance, R. R.; Prock, A.; Silbey, R. Molecular Fluorescence and Energy Transfer Near Interfaces. *Adv. Chem. Phys.* **1978**, *37*, 1–65.
- Swathi, R. S.; Sebastian, K. L. Resonance Energy Transfer from a Dye Molecule to Graphene. *J. Chem. Phys.* **2008**, *129*, 054703/1–9.
- Swathi, R. S.; Sebastian, K. L. Long Range Resonance Energy Transfer from a Dye Molecule to Graphene Has (Distance)<sup>−4</sup> Dependence. *J. Chem. Phys.* **2009**, *130*, 086101/1–3.
- Liu, H.; Ryu, S.; Chen, Z.; Steigerwald, M. L.; Nuckolls, C.; Brus, L. E. Photochemical Reactivity of Graphene. *J. Am. Chem. Soc.* **2009**, *131*, 17099–17101.
- Pisana, S.; Lazzeri, M.; Casiraghi, C.; Novoselov, K. S.; Geim, A. K.; Ferrari, A. C.; Mauri, F. Breakdown of the Adiabatic Born-Oppenheimer Approximation in Graphene. *Nat. Mater.* **2007**, *6*, 198–201.
- Yan, J.; Zhang, Y. B.; Kim, P.; Pinczuk, A. Electric Field Effect Tuning of Electron-Phonon Coupling in Graphene. *Phys. Rev. Lett.* **2007**, *98*, 166802/1–4.
- Wang, G. X.; Yang, J.; Park, J.; Gou, X. L.; Wang, B.; Liu, H.; Yao, J. Facile Synthesis and Characterization of Graphene Nanosheets. *J. Phys. Chem. C* **2008**, *112*, 8192–8195.
- Latil, S.; Henrard, L. Charge Carriers in Few-Layer Graphene Films. *Phys. Rev. Lett.* **2006**, *97*, 036803/1–4.
- Ferrari, A. C.; Meyer, J. C.; Scardaci, V.; Casiraghi, C.; Lazzeri, M.; Mauri, F.; Piscanec, S.; Jiang, D.; Novoselov, K. S.; Roth, S.; Geim, A. K. Raman Spectrum of Graphene and Graphene Layers. *Phys. Rev. Lett.* **2006**, *97*, 187401/1–4.
- Gaskell, P. E.; Skulason, H. S.; Rodenchuk, C.; Szkopek, T. Counting Graphene Layers on Glass via Optical Reflection Microscopy. *Appl. Phys. Lett.* **2009**, *94*, 143101/1–3.